First-order intervalley scattering in low-dimensional systems

Florian Monsef, Philippe Dollfus, Sylvie Galdin, and Arnaud Bournel
Institut d'Électronique Fondamentale, CNRS UMR 8622, Université Paris-Sud, Bâtiment 220, F-91405 Orsay, Cedex, France
(Received 23 January 2002; published 11 June 2002)

The intervalley phonon scattering rate in one- and two-dimensional electron gases is calculated for the case in which the transition matrix element is of first order in the phonon wave vector. This type of interaction is important in silicon at low temperature. The interaction between electrons and bulk phonons is considered in the standard golden rule approach by including the contribution of the components of phonon wave vector in the confinement direction(s). This process makes possible the transition between different subbands, and the resulting total scattering rate differs significantly from the rate commonly used in Si quantum wells.

DOI: 10.1103/PhysRevB.65.212304 PACS number(s): 72.10.Di

I. INTRODUCTION

Intervalley phonon scattering between sixfold-degenerate Δ valleys plays an essential part in the electron transport mechanisms in silicon. Six modes are usually considered in transport modeling to describe this electron-phonon interaction through three *f* and three *g* processes.[1] Regardless of selection rules[2] most authors use a coupling coefficient independent of the phonon wave vector to derive a zero-order transition matrix for all these processes, which yields a conflicting situation. On the one hand, zero-order intervalley processes are forbidden for low-energy phonon modes *f*-TA, *g*-TA and *g*-LA because of symmetry restrictions; and on the other hand, taking into account transitions involving such phonons is required to account for experimental results, especially at low temperature.[3–5] To remedy this inconsistency, Ferry proposed to expand the transition matrix to first order in the phonon wave vector by introducing the coupling coefficient $(D_1 q)^2$ similar to that of intravalley acoustic phonon scattering, where D_1 is a deformation potential having the dimension of energy and q is the phonon momentum.[3] Forbidden transitions then become possible through the first-order term of the transition matrix. This approach has been successfully used to model the electron transport in bulk silicon and silicon devices using the Monte Carlo technique.[6,7]

The same approach may be used to model low-dimensional systems. The purpose of this paper is to carefully derive the scattering rate of first-order process in two-dimensional (2D) and 1D electron gases (2DEG and 1DEG) when considering bulk phonon modes. An expression was initially derived for 2DEG by omitting the coordinate q_z of the phonon wave vector in the confinement direction.[8] However, although both initial and scattered electron wave vectors move in parallel directions, the q_z coordinate must enter the coupling constant and the integration of the square matrix element over all phonon states must include this coordinate, as is usually done for zero-order process and acoustic-phonon scattering both in III-V quantum wells[9,10] and in Si metal-oxide semiconductor field-effect-transistor inversion layers.[11] The momentum conservation indeed is relaxed in the confinement direction, as a consequence of the uncertainty principle.[12] The expression of the scattering rate given in this paper includes the contribution of q_z. It is compared to the previous one for a 2DEG (Sec. II) and extended to a 1DEG (Sec. III).

II. TWO-DIMENSIONAL ELECTRON GAS

All following calculations are made within the framework of the effective mass approximation for a nondegenerate electron gas. The wave function parallel to the interface (*xy* plane) is assumed to be a plane wave and the normalized envelope function in the confinement *z* direction is denoted $\zeta_m(z)$ for the *m*th subband. The first-order matrix element coupling the 2D states $\mathbf{k}$ (on level *l*) and $\mathbf{k}'$ (on level *m*) through a phonon of 3D wave vector $\mathbf{q}$ is then given by

$$|m_{kk'}|^2 = \frac{\hbar^2}{2\rho V \hbar\omega_{i\nu}}\left(N_{i\nu}+\frac{1}{2}\pm\frac{1}{2}\right)D_1^2 q^2 |F_{lm}(q_z)|^2 \times \delta(\mathbf{k}'-\mathbf{k}\pm\mathbf{q}_{xy}), \quad (1)$$

where q_{xy} and q_z are the parallel and normal components of the phonon wave vector, ρ is the crystal density, V the normalization volume, $\omega_{i\nu}$ the phonon angular frequency assumed to be q independent, and $N_{i\nu}$ the phonon number. The upper and lower signs refer to the emission and absorption of a phonon, respectively. The delta function in Eq. (1) arises from the overlap integral in the *xy* plane. It expresses the momentum conservation in this plane, which also implies $q_{xy}^2 = k^2 + k'^2 - 2kk'\cos\theta$, where θ is the scattering angle. The remainder part of the overlap integral is given by

$$F_{lm}(q_z) = \int \zeta_m(z)\exp(iq_z z)\zeta_l(z)dz. \quad (2)$$

By integrating Eq. (1) over the possible phonon states the total square of matrix element becomes

$$|M_{kk'}|^2 = \frac{\hbar^2 D_1^2}{2\rho V\hbar\omega_{i\nu}}\left(N_{i\nu}+\frac{1}{2}\pm\frac{1}{2}\right)\frac{V}{2\pi A}[I_{lm}+J_{lm}], \quad (3)$$

where A is the normalization surface area of the 2DEG. The quantities in brackets are defined by

$$I_{lm} = q_{xy}^2\int |F_{lm}(q_z)|^2 dq_z = 2\pi q_{xy}^2\int \zeta_l(z)^2\zeta_m(z)^2 dz = 2\pi q_{xy}^2 G_{lm}, \quad (4)$$

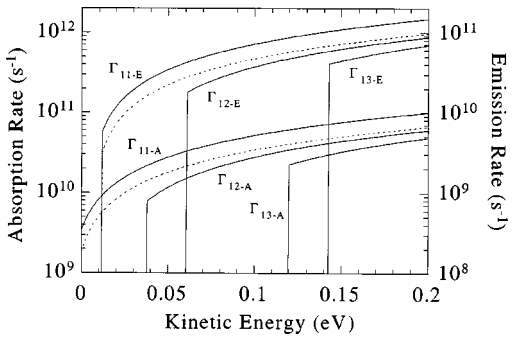

FIG. 1. First-order phonon scattering rates Γ_{1m} vs energy for the lowest subband of a rectangular quantum well at 77 K. The well width is $L=5$ nm. The effective masses are $m_x=m_y=m_t$ and $m_z=m_l$. The subscripts A and E refer to absorption and emission of g-TA phonon ($\hbar\omega_{iv}=11.4$ meV), respectively. The dotted lines indicate the rates $\Gamma_{11\text{-}E}$ (upper curve) and $\Gamma_{11\text{-}A}$ (lower curve) obtained from Eq. (10) derived in Ref. 8. The energies are measured from the bottom of first subband.

$$J_{lm}=\int q_z^2|F_{lm}(q_z)|^2dq_z. \tag{5}$$

The second integral involves the second derivative of delta function,[13] yielding

$$J_{lm}=-\frac{1}{2\pi}\int \rho_{lm}(z)\rho''_{lm}(z)dz=-\frac{1}{2\pi}H_{lm}, \tag{6}$$

where

$$\rho_{lm}(z)=\zeta_l(z)\zeta_m(z) \quad \text{and} \quad \rho''_{lm}(z)=\frac{d^2\rho_{lm}(z)}{dz^2}. \tag{7}$$

For simplicity the energy-momentum relation $\varepsilon(\mathbf{k})$ is assumed to have the parabolic form

$$\varepsilon(\mathbf{k})=\frac{\hbar^2}{2}\left[\frac{k_x^2}{m_x}+\frac{k_y^2}{m_y}\right]. \tag{8}$$

The total probability per unit time Γ_{lm} for an electron to scatter from lth subband to mth subband of another valley is then easily derived from Eq. (3) using the golden rule. By introducing the density of final states $D(\mathbf{k}')=A/4\pi^2$, it is, finally,

$$\Gamma_{lm}(\varepsilon)=\frac{D_1^2}{\rho\hbar^4\omega_{i\nu}}\sqrt{m'_xm'_y}\left(N_{i\nu}+\frac{1}{2}\pm\frac{1}{2}\right)\times\left[(\varepsilon'\sqrt{m'_xm'_y}+\varepsilon\sqrt{m_xm_y})G_{lm}-\frac{\hbar^2}{8\pi^2}H_{lm}\right], \tag{9}$$

where prime superscripts refer to the final valley or final state. The final energy is $\varepsilon'=\varepsilon\mp\hbar\omega-\Delta_{lm}$, where Δ_{lm} is the energy shift between the final and initial subbands. Intervalley scattering rates calculated for 77 K are plotted in Fig. 1 in the simple case of an infinite rectangular quantum well of width $L=5$ nm. The phonon mode considered is g-TA (sometimes denoted $g1$) with an energy $\hbar\omega_{i\nu}=11.4$ meV (Ref. 14) and a deformation potential $D_1=3.0$ eV.[7] Figure 1 shows absorption and emission rates for the lowest subband ($l=1$) of the Δ valley having the longitudinal axis along the confinement direction. In such confinement conditions the transverse mass $m_t=0.1905m_0$ is to be used as the 2D density of states mass $\sqrt{m_xm_y}$ entering Eq. (9) and the longitudinal mass $m_t=0.9163m_0$ is required for the energy-level calculation, yielding five subbands in the energy range considered in Fig. 1.

One may compare Eq. (9) with the results of Ferry obtained without considering q_z in the matrix element calculation. By using the notations of the present work the resulting scattering rate is[8]

$$\Gamma_{lm}(\varepsilon)=\frac{D_1^2}{\rho\hbar^4\omega_{i\nu}}\frac{\sqrt{m'_xm'_y}}{w_m}\left(N_{i\nu}+\frac{1}{2}\pm\frac{1}{2}\right)\times(\varepsilon'\sqrt{m'_xm'_y}+\varepsilon\sqrt{m_xm_y})K_{lm}, \tag{10}$$

where the overlap factor is now

$$K_{lm}=\left[\int \zeta_l(z)\zeta_m(z)dz\right]^2. \tag{11}$$

The normalization thickness w_m introduced in Eq. (10) is chosen as the level width in the z direction. The requirement of such a normalization results from the omission of the q_z contribution to the matrix element. This has the disadvantage of introducing a quantity whose definition is somewhat arbitrary. To calculate the scattering rate [Eq. (10)] to be compared with expression (9), we use the common definition of level extension[15]

$$w_m=\sqrt{\langle z^2\rangle_m-\langle z\rangle_m^2}, \tag{12}$$

where $\langle\alpha\rangle_m$ denotes the average value of α on the mth subband. For the ideal quantum well considered here, the level width w_m is obviously equal to the well width L whatever the subband. The rate Γ_{11} resulting from Eq. (10) is plotted in Fig. 1 (dashed line). All other things being equal, it is about 35% less than the corresponding rate calculated from Eq. (9). This shift, however, depends on the set of wave functions considered for the 2D system and on the definition of the level width. In Eq. (9) the quantity G_{11} may be considered, in fact, as another definition of the inverse of the effective level width of first subband. A more important difference between both models comes from the fact that the overlap factor [Eq. (11)] between equivalent valleys is unity for $l=m$, and vanishes if $l\neq m$, which prohibits the transition unless the initial and final states are in the same subband. In contrast, taking into account the contribution of q_z leads to nonzero overlap integrals (4) and (5), making the coupling between two different subbands non-negligible, as shown in Fig. 1.

The scattering rate [Eq. (9)] may be separated in two terms. The first term (with the overlap factor G_{lm}) involves the contribution of the parallel component q_{xy} of the phonon wave vector to the coupling coefficient, and the second term (with the factor H_{lm}) comes from the q_z contribution. As

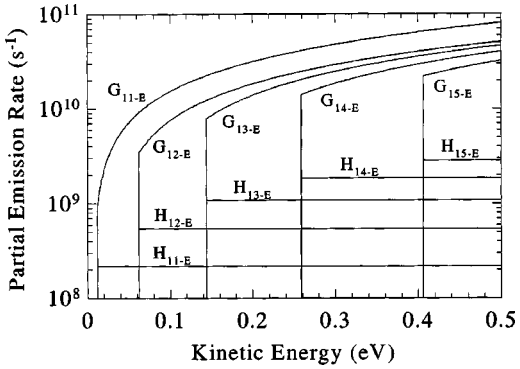

FIG. 2. Partial emission scattering rates vs energy in 2DEG for the same transitions as in Fig. 1 at 77 K. The symbols G_{lm} and H_{lm} refer to the corresponding parts of scattering rates in Eq. (9).

illustrated in Fig. 2 the latter is obviously much smaller than the G_{lm} part, and may be omitted in most relevant cases. It is an expected result arising because of the smallness of the momentum uncertainty due to the confinement in comparison with the momentum transfer for the intervalley scattering. However, the contribution of the H_{lm} term to the scattering rate Γ_{lm} becomes more and more significant when $m-l$ increases, i.e., when the energy separation between initial and final subbands increases.

III. ONE-DIMENSIONAL ELECTRON GAS

In the case of a 1DEG confined in y and z directions and characterized by envelope functions $\zeta_m(y,z)$ the matrix element remains similar to Eq. (1) with a delta function $\delta(\mathbf{k}'-\mathbf{k}\pm\mathbf{q}_x)$ that expresses the momentum conservation in the x direction only. The overlap integral F_{lm} now depends on both q_y and q_z components:

$$F_{lm}(q_y,q_z)=\int \zeta_m(y,z)\exp(iq_y y)\exp(iq_z z)\zeta_l(y,z)dy\,dz. \tag{13}$$

The derivation of the total matrix element $M_{kk'}$ still involves quantities G_{lm} and H_{lm} now defined by

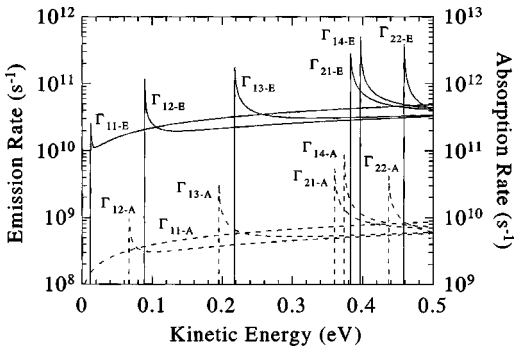

FIG. 3. First-order phonon scattering rates vs energy for the lowest subband in a square quantum wire of side 5 nm at 77 K. Unlike in Eq. (17), the quantity Γ_{ij} here refers to the scattering rate between the lowest subband 11 and the final subband ij. The energies are measured from the bottom of first subband.

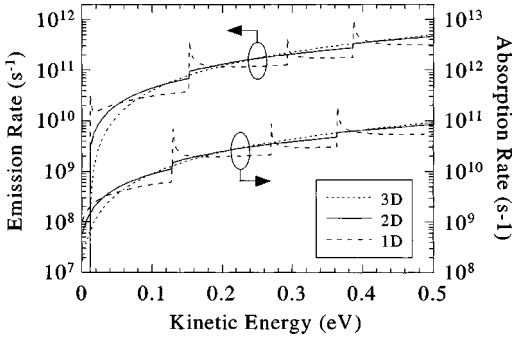

FIG. 4. Total emission and absorption scattering rates vs energy at 77 K for the lowest subband in square quantum well (solid lines) and wire (dashed lines) of thickness 5 nm. The dotted lines indicate the rates in three-dimensional gas. An isotropic mass is considered.

$$G_{lm}=\int \zeta_l(y,z)^2\zeta_m(y,z)^2dy\,dz, \tag{14}$$

$$H_{lm}=\int \rho_{lm}(y,z)\left[\frac{\partial^2\rho_{lm}(y,z)}{\partial y^2}+\frac{\partial^2\rho_{lm}(y,z)}{\partial z^2}\right]dy\,dz, \tag{15}$$

where

$$\rho_{lm}(y,z)=\zeta_l(y,z)\zeta_m(y,z). \tag{16}$$

The derivation of the total probability per unit time Γ_{lm} for an electron to scatter from the lth subband to the mth subband of another valley is straightforward. For parabolic bands one obtains

$$\Gamma_{lm}(\varepsilon)=\frac{\sqrt{2}D_1^2}{\rho\hbar^3\omega_{i\nu}}\left(N_{i\nu}+\frac{1}{2}\pm\frac{1}{2}\right)\frac{\sqrt{m_x'}}{\sqrt{\varepsilon'}}\times\left[(\varepsilon' m_x'+\varepsilon m_x)G_{lm}-\frac{\hbar^2}{8\pi^2}H_{lm}\right]. \tag{17}$$

As for most scattering processes in a 1DEG, the 1D density of states generates a divergence of the scattering rate near threshold energy $\varepsilon'=0$. It is a consequence of the semiclassical expression of energy conservation. It vanishes if the rigorous q dependence in the matrix element is included, e.g., by calculating the self-energy of the electron-phonon interaction to account for the collisional broadening effect.[16] Convenient averaging techniques have been used to avoid the divergence in semiclassical transport calculation.[17]

Scattering rates calculated from Eq. (17) are plotted in Fig. 3 for the lowest subband of an infinite square quantum wire of side 4 nm. The effective masses in the confinement directions are $m_y=m_t$ and $m_z=m_l$, which yield six subbands in the energy range considered. Each subband is defined by a pair of quantum numbers, but to simplify the notations we only indicate in subscript the final pair of numbers in Fig. 1. Similarly to the 2DEG case the second term (with H_{lm}) coming from the contribution of q_y and q_z components is much smaller than the main part.

One may now compare the 1D and 2D scattering rates [Eqs. (9) and (17)] with the 3D ones.[3] To make the comparison more significant we use a unique isotropic mass $m=(m_l m_t^2)^{1/3}$, so that the results are independent on the confinement direction. The width of both the quantum well and quantum wire is now 5 nm. For the same phonon as in previous figures, the total absorption and emission rates in the lowest subband are plotted in Fig. 4, together with the corresponding 3D rates. The 1D rates (dashed lines) and 2D rates (solid lines) are piecewise approximations of the 3D rates (dotted lines) due to discontinuities in the final density of low-dimensional states. This satisfying result cannot be obtained if the coordinates of the phonon wave vectors in confinement directions are omitted, as in Eq. (10). Finally, one can easily verify that the 1D, 2D, and 3D total rates turn out to be all the closer as the confinement width becomes thicker.

IV. CONCLUSION

The first-order intervalley phonon scattering rate has been derived using the conventional approach of the Fermi golden rule. Including the contribution of the component(s) of phonon wave vector in the confinement direction enables the transition if the initial and final states are not in the same subband, which is impossible through the commonly used approach of this scattering mechanisms in Si quantum wells. The resulting total scattering rates in 1DEG and 2DEG are very consistent with the corresponding rates in a bulk system.

ACKNOWLEDGMENTS

The authors would like to thank Johann Sée for helpful discussions.

[1] C. Canali, C. Jacoboni, F. Nava, G. Ottaviani, and A. Alberigi-Quaranta, Phys. Rev. B **12**, 2265 (1975).
[2] H. W. Streitwolf, Phys. Status Solidi **37**, K47 (1970).
[3] D. K. Ferry, Phys. Rev. B **14**, 1605 (1976).
[4] J. C. Portal, L. Eaves, S. Askenazy, and R. A. Stradling, Solid State Commun. **14**, 1241 (1974).
[5] C. Hamaguchi, Physica B & C **134**, 87 (1985).
[6] T. Yamada, J. R. Zhou, H. Miyata, and D. K. Ferry, IEEE Trans. Electron Devices **ED 41**, 1513 (1994).
[7] P. Dollfus, J. Appl. Phys. **82**, 3911 (1997).
[8] D. K. Ferry, Surf. Sci. **57**, 218 (1976).
[9] S. M. Goodnick and P. Lugli, Phys. Rev. B **37**, 2578 (1988).
[10] C. Jacoboni and P. Lugli, *The Monte Carlo Method for Semiconductor Device Simulation* (Springer-Verlag, Wien, 1989).
[11] M. V. Fischetti and S. E. Laux, Phys. Rev. B **48**, 2244 (1993).
[12] B. K. Ridley, J. Phys. C **15**, 5899 (1982).
[13] M. Abramowitz and I. A. Stegun, *Handbook of Mathematical Functions* (Dover, New York, 1972), p. 1020.
[14] M. Asche and O. G. Sarbei, Phys. Status Solidi B **103**, 11 (1981).
[15] K. Yamasaki, T. Ezaki, N. Mori, and C. Hamaguchi, Inst. Phys. Conf. Ser. No. 162 (IOP Publishing, Bristol, UK, 1999), Chap. 7. p. 313.
[16] S. Briggs, B. A. Mason and J. P. Leburton, Phys. Rev. B **40**, 12001 (1989).
[17] Y. Ando and A. Cappy, J. Appl. Phys. **74**, 3983 (1993).